



**Please cite the Published Version**

Algolfat, Amna, Wang, Weizhuo  and Albarbar, Alhussein  (2023) Damage identification in complex structures using vibration data. In: 2023 3rd International Conference on Electrical, Computer, Communications and Mechatronics Engineering (ICECCME), 19 July 2023 - 21 July 2023, Tenerife, Canary Islands, Spain.

**DOI:** <https://doi.org/10.1109/ICECCME57830.2023.10252757>

**Publisher:** IEEE

**Version:** Accepted Version

**Downloaded from:** <https://e-space.mmu.ac.uk/632913/>

**Usage rights:**  In Copyright

**Additional Information:** © 2023 IEEE. Personal use of this material is permitted. Permission from IEEE must be obtained for all other uses, in any current or future media, including reprinting/republishing this material for advertising or promotional purposes, creating new collective works, for resale or redistribution to servers or lists, or reuse of any copyrighted component of this work in other works.

**Enquiries:**

If you have questions about this document, contact [openresearch@mmu.ac.uk](mailto:openresearch@mmu.ac.uk). Please include the URL of the record in e-space. If you believe that your, or a third party's rights have been compromised through this document please see our Take Down policy (available from <https://www.mmu.ac.uk/library/using-the-library/policies-and-guidelines>)

# Damage identification in complex structures using vibration data

Amna Algotfat

*Smart Infrastructure and Industry  
Research Group, Department of Engineering,  
Manchester Metropolitan University,  
Manchester M1 5GD, UK  
amnaalgotfat@hotmail.com*

Weizhuo Wang

*Smart Infrastructure and Industry  
Research Group, Department of Engineering,  
Manchester Metropolitan University,  
Manchester, M1 5GD UK  
W.Wang@mmu.ac.uk*

Alhussein Albarbar

*Smart Infrastructure and Industry  
Research Group, Department of Engineering,  
Manchester Metropolitan University,  
Manchester M1 5GD, UK  
A.Albarbar@mmu.*

**Abstract—** This study presents a damage identification procedure for complex structures based on analysing changes in vibration data between healthy and damaged conditions. The procedure involves calculating and comparing the first six mode shapes of both the intact and damaged structures using finite element analysis. The case study of 5Mega Watt National Renewable Energy Laboratory offshore wind turbine blade has been used to demonstrate the application of the procedure. The main objective is to utilise this procedure to identify and evaluate the severity of damage in different scenarios. Additionally, the procedure can be applied at various stages to detect and identify early signs of damage, serving as an early warning system.

**Keywords—** damage identification, vibration data, dynamic characteristics, wind turbines.

## I. INTRODUCTION

Numerous methods have been introduced for damage identification by analysing modal parameters. Damage indices techniques are employed to assess and compare the structural condition of both healthy and damaged structures. [1]. The modal parameters include the natural frequencies, mode shapes, mode shape curvature, and strain energy. These vibration data can be implemented as damage indices to investigate the health performance of the complex structure and evaluate its reliability. The study in [2] focuses on utilising vibration based information to examine the presence of discontinuities in the curvature curve. The methodology was based on physical changes of smoothness that manifest themselves by increasing deviations in modal parameters such as the eigen values. The investigation involves a damaged blade, where the variations in the curvature curve is analysed by considering changes within the proposed sections. By assessing these changes in curvature, the study aims to identify and characterise the damage within the beam structure. The procedure in [3] utilises the elementary eigen vector as a damage indicator to assess the health state of the studied beam. It defines a damage index based on the first eigenvalue vector.

A similar technique in [4] is employed, where the change in system frequencies due to variations in bending stiffness is examined. The study assumes a linear relationship between frequency changes and the degree of damage. The approach in [5] relies on the concept that the ratio between local and global strain energy remains constant before and after damage, assuming negligible damage. This enables damage assessment by analysing the strain energy distribution in the structure. According to [6], considering the relationship between strain energy, curvature integrals, and the contribution of all power modes can enhance the performance of the damage index for linear structures. In [7], modal strain energy is used as a damage index to detect early local damage along the structure span. The local modal matrix of each blade section is utilised to calculate the strain energy index for each corresponding mode, enabling the identification and assessment of damage at different locations along the blade.

The paper presents a computationally efficient finite element model that generates a dynamic model for evaluating the dynamic modal characteristics of a horizontal axis wind turbine (HAWT) blade. The proposed framework monitors, diagnoses, predicts, and identifies early-stage damage by comparing data from intact and damaged conditions. The key focus of the framework lies in integrating diverse models and various source data to enhance the reliability of wind turbines.

## II. A. STRUCTURAL MODELLING

In this study, Rayleigh beam theory is adopted to derive the equation of motion. The effect of different deformations is included to study their effect on the free vibration analysis. The governing equation of motion for the 5MW HAWT blade in the out-of-plane direction is determined as [8]:

$$\rho A(x) \frac{\partial^2 w}{\partial t^2} + \frac{\partial^2}{\partial x^2} \left( E I_{zz}^*(x) \frac{\partial^2 w}{\partial x^2} \right) - \frac{\partial}{\partial x} \left( T(x) \frac{\partial w}{\partial x} \right) - \frac{\partial}{\partial x} \left( \rho I_{zz}^*(x) \frac{\partial^3 w}{\partial x \partial t^2} \right) + \Omega^2 \frac{\partial}{\partial x} \left( \rho I_{zz}^*(x) \frac{\partial w}{\partial x} \right) - k(x)w = f(x, t)$$

(1)

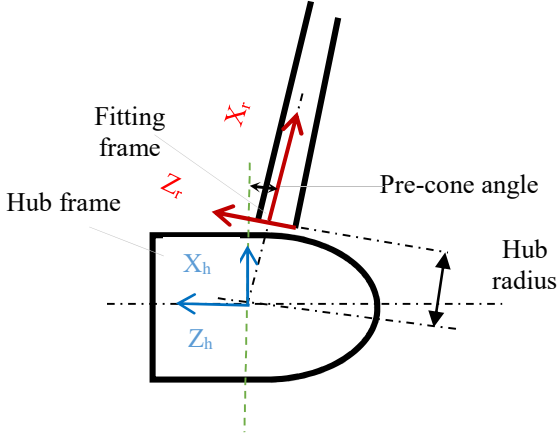


Fig. 1. Root coordinate frames of 5MW NREL blade.

where  $T(x)$  represents the axial force resulting from the combined effects of centrifugal and gravitational forces acting on the system. This force is measured at a specific distance  $x$  from the center of rotation.

$$T(x, t) = T_c(x) + T_g(x, t)$$

$$T(x, t) = \frac{1}{2} \int_x^L [(\rho(x)A(x)\Omega^2(R + x \cos(\phi)) - \rho(x)A(x)g \cos(\theta) \cos(\phi))] dx \quad (2)$$

$I^* = I(x)\cos^2(\phi)$  and  $\phi$  is the pre-cone angle

$$k(x) = \frac{1}{2} \int_0^L \left[ -\frac{1}{8} \rho A(x) \Omega^2 (2 \cos(2\phi) + \cos(2(\phi - \theta_p))) + 2 \cos(2\theta_p) + \cos(2(\phi + \theta_p)) - 6 \right] w(x, t)^2 dx \quad (3)$$

Equation (3) represents the effects of control angles effect (pre-cone and pitch angles) [8]:

### B. Finite element model

The matrix equation of the blade under different excitation forces is [9]:

$$[M]\ddot{X} + [C]\dot{X} + [K]X = \begin{Bmatrix} F_1(r, t) \\ F_2(r, t) \\ F_3(r, t) \\ \vdots \\ F_n(r, t) \end{Bmatrix} \quad (4)$$

where,  $X, \dot{X}, \ddot{X}$  represent the vectors of displacement, velocity, and acceleration, respectively.  $F$  represents the various excitation loads in the flap-wise direction that influence the system.  $M, C,$  and  $K$  in the left hand side of the equation represent the local mass, local damping, and local stiffness matrices. The parameter  $r$  represents the radius at each certain section from 1 to  $n$ .

The undamaged local modal matrices are composed of elements of [10]:

$$M_{ij} = \int_0^L \rho(x)A(x)\varphi_j(x)\varphi_i(x) dx + \int_0^L \rho(x)I(x) \frac{\delta\varphi_j}{\delta x} \frac{\delta\varphi_i}{\delta x} dx \quad (5)$$

$$K_{ij} = \int_0^L EI^*(x) \frac{\delta^2\varphi_i(x)}{\delta x^2} \frac{\delta^2\varphi_j(x)}{\delta x^2} dx + \int_0^L T(x, t) \frac{\delta\varphi_i}{\delta x} \left( \frac{\delta\varphi_j}{\delta x} \right) dx - \int_0^L k(x)\varphi_j\varphi_i dx - \int_0^L \Omega^2 \rho(x)I^*(x) \frac{\delta\varphi_i}{\delta x} \left( \frac{\delta\varphi_j}{\delta x} \right) dx \quad (6)$$

### C. Damage modelling

The damage can be assumed as a loss of local rigidity at any blade section. This can be implemented by assuming a scalar  $\beta$  to qualify the reduction in the local rigidity[1]. The damage severity can be addressed by choosing a parameter  $p$ , where  $p = 1 - \beta$  and  $\beta \in (0,1]$ . The local stiffness matrix is recalculated with changes in the damage parameter  $p$ .

When the value of  $\beta$  is set to 0, it signifies the intact stiffness value. As an illustration, if a 2% reduction in stiffness from the intact value is selected for element 10, which corresponds to aerofoil DU21\_A1 and is positioned at a distance of 32.8m from the blade root, the stiffness matrix for this section will be modified as follows:  $K_{10} = pK = (1 - 0.02)K$ , where  $K$  represents the intact stiffness matrix. Table I provides an overview of the seven different blade sections and the corresponding cylinders and aerofoil types [11]. Additionally, Fig.2 showcases the proposed NREL blade.

TABLE I. BLADE SECTIONS AND AEROFOIL DISTRIBUTION OF 5MW NREL WIND TURBINE.

Section	Airfoil	Section Length (m)
1	Cylinder 1	2.7333
2	Cylinder 1	2.7333
3	Cylinder 2	2.7333
4	DU40_A17	4.1000
5	DU35_A17	4.1000
6	DU35_A17	4.1000
7	DU30_A17	4.1000
8	DU25_A17	4.1000
9	DU25_A17	4.1000
10	DU21_A17	4.1000
11	DU21_A17	4.1000
12	NACA_64_618	4.1000
13	Same as above	4.1000
14	Same as above	4.1000
15	Same as above	2.7333
16	Same as above	2.7333
17	Same as above	2.7333

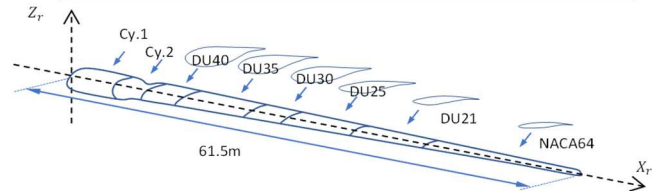


Fig. 2. The locations of the blade sections from the blade's root. The sections lengths are: 8.2+ 4.1+ 8.2+ 4.1+ 8.2+8.2+20.1= 61.5 m.

### III. DAMAGE IDENTIFICATION

The generalised eigenvalue problem for each element with mass and stiffness matrices may be written as [1]:

$$[K - \lambda_i M]z_j^i = 0 \quad (7)$$

where  $\lambda_i$  represents the eigenvalue at mode  $i$ , and  $z_j^i$  is the relevant mode-shape displacement at the  $j^{th}$  degree of freedom. Assuming that damage reduces the local stiffness matrix, it consequently alters the modal frequencies and corresponding mode shapes, expressed as

$$[(K + \Delta K) - (\lambda_i + \Delta \lambda)M](z^i + \Delta z^i) = 0 \quad (8)$$

and

$$\Delta \lambda_i = z^{(i)T} \Delta K z^{(i)} \quad (9)$$

$$\Delta z^{(i)} = \sum_{j=1}^N \frac{z^{(j)T} \Delta K z^{(i)}}{\lambda_i - \lambda_j} \quad (10)$$

which indicate the variation in mode shape displacements and the structural frequencies due to the undamaged structure. The local damaged stiffness matrix damaged natural frequencies, and mode shapes can be recalculated based on their corresponding intact values as follows [12]:

$$K_i^d = K_i + \beta_i K_i \quad \text{and} \quad -1 < \beta_i < 0 \quad (11)$$

$$\omega_i^d = \omega_i + \Delta \omega_i \quad (12)$$

$$z_i^d = z_i + \Delta z_i \quad (13)$$

#### IV. COMPARISON AND CORRELATION BETWEEN MODE SHAPES

##### A. Modal Assurance Criterion (MAC)

The MAC can be a damage index to quantify the correlation between pairs of mode shapes, specifically between the intact mode shape and its damaged matching part. It is computed as the inner product of the eigen vectors  $\Psi_A$  and  $\Psi_B$  [12]:

$$MAC(A, B) = \frac{|\{\Psi_A\}_n^T \{\Psi_B\}_m|^2}{(\{\Psi_A\}_n^T \{\Psi_A\}_n)(\{\Psi_B\}_m^T \{\Psi_B\}_m)} \quad (14)$$

##### B. Auto Modal Assurance Criterion (AutoMAC)

The MAC damage index results can be influenced by the number of degrees of freedom considered in the analysis. However, factors like aliasing and insufficient data points can also hinder the correlation and discrimination between mode shapes. To address these issues, a version of MAC called AutoMAC is utilised. In AutoMAC plots, the diagonal values are expected to be unity as each displacement vector perfectly correlates with itself. The AutoMAC matrix should be symmetric [13], with non-zero off-diagonal terms depending on the selected degrees of freedom.

##### C. Frequency-scaled MAC (FMAC)

To build a comprehensive interpretation of the full correlation between any pair of mode shapes, it is necessary to plot a comparison diagram of natural frequency values and MAC values. In this diagram, the mode number scale of MAC replaces the values of the natural frequency at each value being compared. This method makes it easier to make a clear judgment about the level of correlation between the compared models [13]

#### V. SIMULATION OUTCOMES

The specifications of 5 Mega Watt NREL offshore wind turbine blade is used as a benchmark. The blade is divided into 17 sections based on the aerofoils, as presented in Table I. The

blade's hub diameter is approximately 3 m, the rotor radius is 63 m, and the rotor speed is 12.1 RPM [11]. Table II presents the first five eigen values of the model in the flap-wise and edge-wise directions. Next, a comparison is made between the natural frequencies obtained in this study and those reported in the literature using the same NREL 5 MW HAWT blade geometry and material properties, specifically by the B-Modes and FAST codes [11], Li et al. [14], and Jeong et al. [15] and [16]. Fig 3 displays the first six healthy mode shapes compared to their damaged counterparts affected by a 15% stiffness reduction concentrated at 32.8 m from the hub.

TABLE II. THE NATURAL FREQUENCIES OF THE FIRST 5 MODES, INCLUDING THE FLAP-WISE (FL) AND EDGE-WISE (ED) DIRECTIONS OF A SINGLE BLADE

NO	Present work (Hz)	B Modes Hz [NREL]	FAST Hz [NREL]	Li Z et al., (Hz)	Jeong et al., (Hz)
1	0.68 FL	0.69 FL	0.68 FL	0.67 FL	0.68 FL
2	1.11 ED	1.12 ED	1.10 ED	1.11 ED	1.10 ED
3	1.98 FL	2.00 FL	1.94 FL	1.92 FL	1.98 FL
4	4.10 ED	4.12 ED	4.00 ED	3.96 ED	3.99 ED
5	4.54 FL	4.69 FL	4.43 FL	4.43 FL	4.66 FL

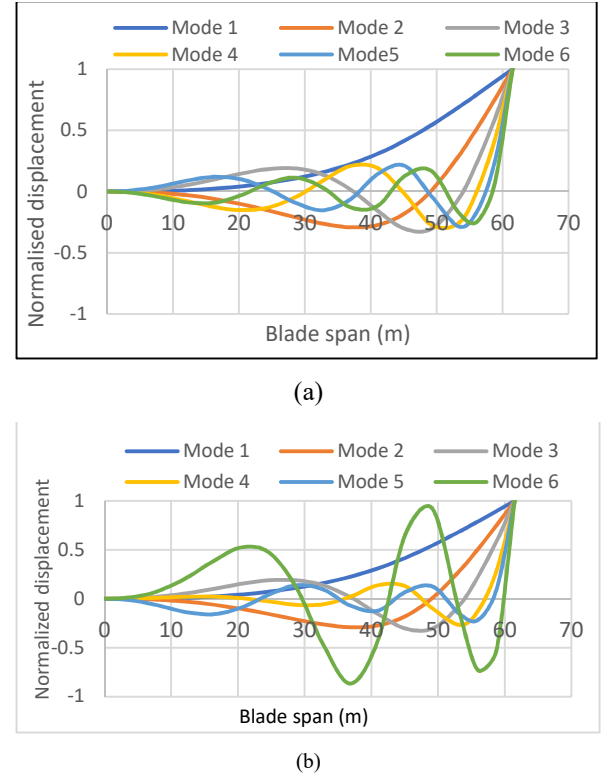


Fig. 3. First six mode shapes a. Healthy blade, b. Damaged blade at stiffness reduction by 15% at blade length 32.8m.

Figs. 4a and 4b illustrate the correlation analysis of the healthy blade's first six sets of translational and angular mode shapes using the AutoMAC index. These plots help determine the appropriate number of degrees of freedom for correlation and validate the MAC index as an indicator. It can be observed that

there is a nearly perfect correlation among the selected mode shapes for the healthy blade.

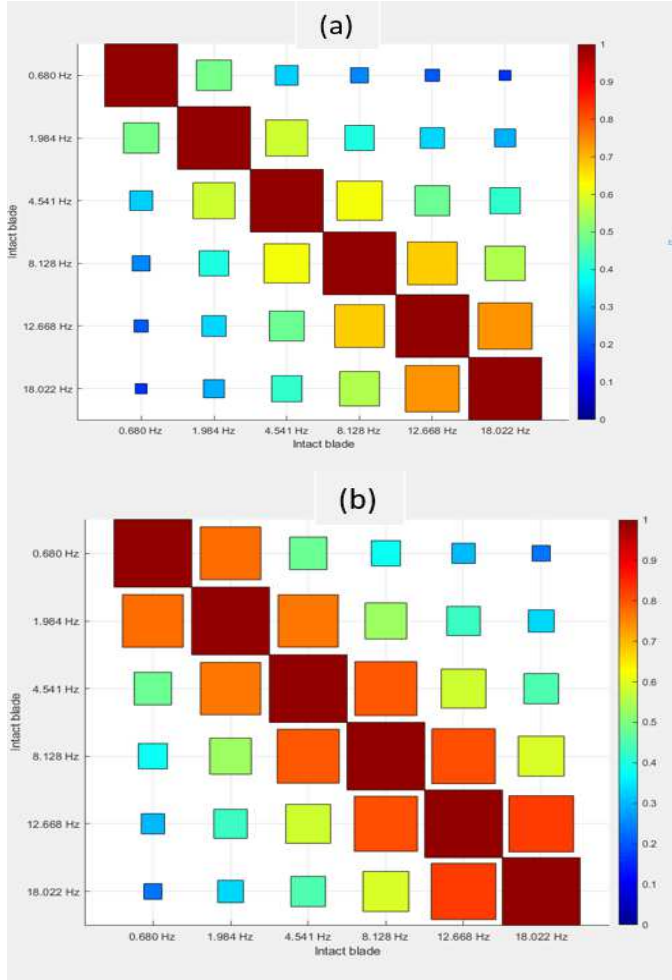


Fig. 4. AutoMAC index for healthy blade of modes 1 to 6, (a), translational modes and (b), angular modes.

Figs 5a and 5b display the MAC index values for the first six mode shapes comparing the intact blade with its damaged counterpart. The plots represent the translational and angular displacements. It is evident that there is poor correlation between the intact and damaged blades, particularly for the fourth mode shape after mode 1. The damage in this case involves a 20% reduction in stiffness concentrated at a distance of 32.8m from the blade root. The MAC values indicate a lack of correlation between the translation and angular mode shapes, suggesting poor agreement between the intact and damaged configurations.

Fig. 6 presents a comparison of the first five mode shapes using three damage indices within the same plot. It includes the eigen values of the intact model versus its damaged counterpart at a 20% rigidity reduction from the undamaged one. Additionally, it incorporates the AutoMAC values of the intact blade and the MAC values between the intact and damaged blades. The plot highlights the differences between the intact frequency curve (represented by a solid black line) and the damaged frequency curve (represented by a dotted black line). The coloured curves represent the first five MAC values, while the dashed curves

represent the AutoMAC values. The variations between the paired curves indicate the impact of damage and its distribution along the blade span.

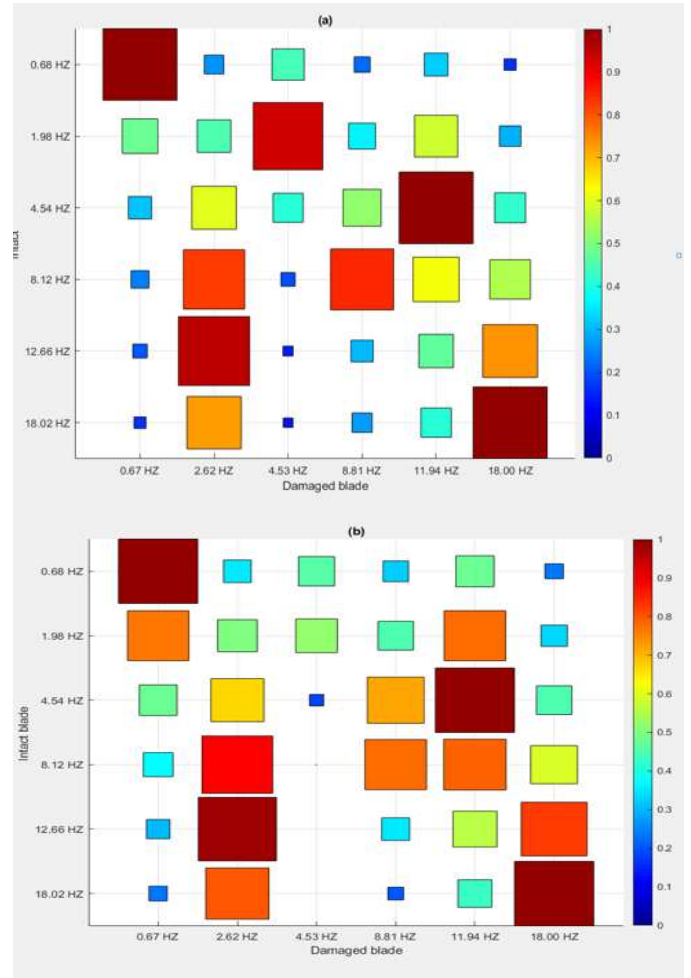


Fig. 5. MAC index values for the six mode shapes between of the undamaged 5MW blade and its destroyed counterpart. The damage scenario involves a 20% reduction in stiffness at a distance of 32.8m from the blade root. The MAC index is computed separately for (a) translational modes and (b) angular modes.

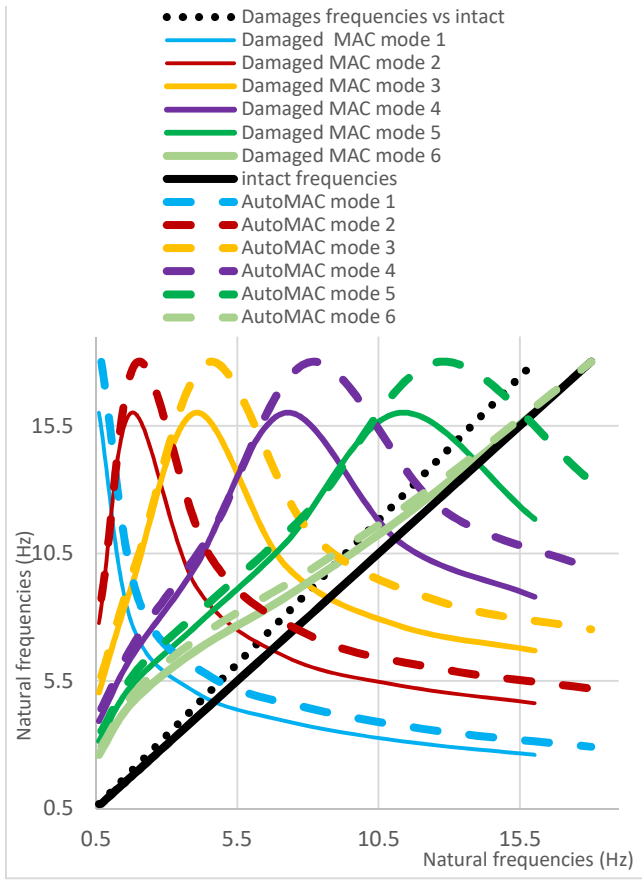


Fig. 6. comparison of MAC and AutoMAC using the first ten natural frequencies and the first six mode shapes of the intact NREL 5 MW blade and damaged pair. The damage scenario involves a 20% reduction in stiffness in the flap-wise direction.

## VI. CONCLUSION

This paper focused on the detection and diagnosis of damage in offshore wind turbine blades using a vibration-based technique. The modal parameters were utilised to analyse the behavior of a specific 5 MW blade developed by NREL, which served as the reference model. By extracting the health model parameters from the intact blade, a baseline was established for assessing damage severity. The objective was to establish a reliable comparison between the healthy complex structure and its destroyed counterpart. Damage indices were employed for a direct and objective comparison of dynamic modal properties. In particular, the MAC index proved to be a sensitive indicator for complex structures like offshore wind turbine blades. Any deviations observed in the vibration data, including frequencies and mode shapes, between the intact and damaged blades were utilised to identify the presence of damage, determine its location, and assess its severity. This approach facilitated effective detection and evaluation of damage in offshore wind turbine blades.

## REFERENCES

- [1] A. Algolfat, W. Wang, A. Albarbar. The sensitivity of 5MW wind turbine blade sections to the existence of damage. *Energies*. 2023 Jan 28;16(3):1367.
- [2] V.B. Dawari, GR. Vesmawala. Structural damage identification using modal curvature differences. *IOSR Journal of Mechanical and Civil Engineering*. 2013;4:33-8. K. Elissa, "Title of paper if known," unpublished.
- [3] R.Gorgin. Damage identification technique based on mode shape analysis of beam structures. *InStructures 2020 Oct 1 (Vol. 27, pp. 2300-2308)*. Elsevier.
- [4] U. Galvanetto, G. Violaris. Numerical investigation of a new damage detection method based on proper orthogonal decomposition. *Mechanical Systems and Signal Processing*. 2007 Apr 1;21(3):1346-61.
- [5] P. Cornwell, SW. Doebling, CR. Farrar. Application of the strain energy damage detection method to plate-like structures. *Journal of sound and vibration*. 1999 Jul 8;224(2):359-74.
- [6] S.E.Fang, R. Perera. Power mode shapes for early damage detection in linear structures. *Journal of Sound and Vibration*. 2009 Jul 10;324(1-2):40-56.
- [7] M.M. Rezaei, M. Behzad, H. Moradi, H. Haddadpour. Modal-based damage identification for the nonlinear model of modern wind turbine blade. *Renewable energy*. 2016 Aug 1; 94:391-409.
- [8] A. Algolfat, W. Wang, A. Albarbar. Comparison of beam theories for characterisation of a NREL wind turbine blade flap-wise vibration. *Proceedings of the Institution of Mechanical Engineers, Part A: Journal of Power and Energy*. 2022 Nov;236(7):1350-69.
- [9] A. Algolfat, W. Wang, A. Albarbar. Study of centrifugal stiffening on the free vibrations and dynamic response of offshore wind turbine blades. *Energies*. 2022 Aug 23;15(17):6120.
- [10] A. Algolfat, W. Wang, A. Albarbar. Dynamic responses analysis of a 5MW NREL wind turbine blade under flap-wise and edge-wise vibrations. *Journal of Dynamics, Monitoring and Diagnostics*. 2022 Sep 13:208-22.
- [11] J. Jonkman, S. Butterfield, W. Musial, G. Scott. Definition of a 5-MW reference wind turbine for offshore system development. *National Renewable Energy Lab.(NREL), Golden, CO (United States)*; 2009 Feb 1
- [12] J.T.Kim, N. Stubbs. Improved damage identification method based on modal information. *Journal of Sound and Vibration*. 2002 Apr 25;252(2):223-38.
- [13] D.J.Ewins. *Modal testing: theory, practice and application*. John Wiley & Sons; 2009 Jul 20.
- [14] Z.Li, B. Wen, X. Dong, Z. Peng, Y. Qu, W. Zhang. Aerodynamic and aeroelastic characteristics of flexible wind turbine blades under periodic unsteady inflows. *Journal of Wind Engineering and Industrial Aerodynamics*. 2020 Feb 1; 197:104057.
- [15] M.S.Jeong, M.C.Cha, S.W. Kim, I. Lee, T. Kim. Effects of torsional degree of freedom, geometric nonlinearity, and gravity on aeroelastic behaviour of large-scale horizontal axis wind turbine blades under varying wind speed conditions. *Journal of Renewable and Sustainable Energy*. 2014 Mar 25;6(2):023126.
- [16] A. Algolfat, A. Albarbar, W. Wang. Dynamic Modelling of Wind Turbine Structure for Health Monitoring. *InInternational Virtual Conference on Industry 4.0: Select Proceedings of IVCIA. 0 2021 2023 Apr 1 (pp. 185-195)*. Singapore: Springer Nature Singapore.